methods

Detergent-free isolation and characterization of cholesterol-rich membrane domains from *trans*-Golgi network vesicles

Mark G. Waugh,[1] K. M. Emily Chu, Emma L. Clayton, Shane Minogue, and J. Justin Hsuan

Centre for Molecular Cell Biology, Department of Inflammation, Division of Medicine, University College London, Royal Free Campus, Rowland Hill Street, London, United Kingdom NW3 2PF

Abstract **Cholesterol is an abundant lipid of the *trans*-Golgi network (TGN) and of certain endosomal membranes where cholesterol-rich microdomains are important in the organization and compartmentalization of vesicular trafficking. Here we describe the development of a rapid method to isolate a cholesterol-rich endomembrane fraction. We show that widely used subcellular fractionation techniques incompletely separate cholesterol-rich membranes, such as the TGN, from organelles, such as late endosomes and lysosomes. To address this issue, we devised a new subcellular fractionation scheme involving two rounds of velocity centrifugation, membrane sonication, and discontinuous sucrose density gradient centrifugation. This strategy resulted in the isolation of a cholesterol and GM1 glycosphingolipid-enriched membrane fraction that was completely cleared of plasma membrane, endoplasmic reticulum, and mitochondria. This buoyant fraction was enriched for the TGN and recycling endosome proteins Rab11 and syntaxin-6, and it was well resolved from *cis*-Golgi and early and late endosomal membranes. We demonstrate that this technique can give useful insights into the compartmentation of phosphoinositide synthesis, and it facilitates the isolation of cholesterol-rich membranes from a population of TGN-trafficking vesicles.**—Waugh, M. G., K. M. E. Chu, E. L. Clayton, S. Minogue, and J. J. Hsuan. **Detergent-free isolation and characterization of cholesterol-rich membrane domains from *trans*-Golgi network vesicles. *J. Lipid Res.* 2011.** 52: **582–589.**

Supplementary key words caveolae • cholesterol/cell tissue • fluorescence microscopy • Golgi apparatus

Cholesterol is known to be enriched in the membranes of recycling endosomes (1), late endosomal multivesicular bodies (2), and the *trans*-Golgi network (TGN). Large increases in endosomal cholesterol levels are a feature of some inherited lysosomal lipid storage disorders, such as Niemann Pick disease (3–5), where mutations to the Niemann Pick Type C protein result in reduced lipoprotein-derived cholesterol egress and, consequently, an enlarged late-endosomal phenotype. This lipid storage defect induces aberrant vesicular trafficking due to cholesterol-dependent inhibition of several endosomal Rab GTPases, including Rab4 (6), Rab7 (7, 8), Rab8 (9), and Rab9 (8, 10). Augmented intracellular cholesterol concentrations also feature in the formation of macrophage-derived foam cells in atherosclerotic lesions (11), and increased intracellular cholesterol synthesis promotes mitogenesis of androgen-sensitive prostate cancer cells (12). On the other hand, there is also evidence that decreased cholesterol synthesis in response to statin treatment can modulate intracellular vesicular trafficking pathways (13, 14). Therefore, insights into the composition and function of cholesterol-rich endomembranes are likely to further our understanding of multiple disease-associated, intracellular-trafficking pathways.

Despite the importance of lipid microdomains in Golgi-endosomal trafficking, there are no available techniques to easily isolate cholesterol-rich endomembranes. Current strategies to isolate membrane microdomains from whole-cell lysates take advantage of characteristic properties, such as detergent insolubility and low buoyant density, to facilitate their purification on either sucrose or Optiprep gradients (reviewed in Ref. 15). Although widely employed, these methods tend to give rise to heterogeneous membrane preparations (15) that may also contain membrane fragments from mitochondria (16). The isolation of endosomal

This work was supported by Cancer Research UK Grant C25540/A8562 (M.G.W., K.M.E.C., and J.J.H.) and Biotechnology and Biological Sciences Research Council (BBSRC) Grant BB/G021163/1 (S.M., E.C., and M.G.W.).

Manuscript received 11 November 2010 and in revised form 16 December 2010.

Published, JLR Papers in Press, December 29, 2010
DOI 10.1194/jlr.D012807

Abbreviations: ER, endoplasmic reticulum; ERC, endosomal recycling compartment; PI, phosphatidylinositol; PI4P, phosphatidylinositol 4-phosphate; PI4K, phosphatidylinositol 4-kinase; PI4KII, type II phosphatidylinositol 4-kinase; PNS, postnuclear supernatant; TGN, *trans*-Golgi network.

[1]To whom correspondence should be addressed.
e-mail: m.waugh@medsch.ucl.ac.uk

and TGN lipid microdomains is complicated by the fact that these membranes are intrinsically of low buoyant density (17). In equilibrium sucrose density gradients, endosomal and TGN membranes often float to the 20-30% sucrose layer interface (17), which is often the region in which caveolae and other low-buoyant-density plasma membrane microdomains are found (18, 19). One way around this problem would be to isolate an endosome-rich membrane fraction prior to preparing microdomains. However, this tends to involve at least one density gradient procedure which can be technically difficult and may only achieve partial separation of intracellular vesicles from the plasma membrane. In this study, we describe a simple centrifugal preclearance step that takes 20 min and leads to the pelleting of all immunoreactivity against abundantly expressed markers for the endoplasmic reticulum, plasma membrane, and mitochondria, together with about 70% of the total cellular cholesterol content. The resultant supernatant is then subjected to sonication, carbonate extraction, and discontinuous sucrose gradient centrifugation similar to the method of microdomain isolation originally described by Song et al. (18). We show that this membrane preparation contains a pool of cholesterol, phosphatidylinositol 4-phosphate (PI4P), and markers for the TGN and endosomal recycling compartment.

MATERIALS AND METHODS

Materials

Anti-EEA1, anti-LAMP-1, Anti-Rab11, anti-syntaxin 4, anti-syntaxin-8, and anti-syntaxin-6 were from BD Biosciences (Oxford, UK). Protease inhibitor cocktail tablets (Complete™, without EDTA) were from Roche Diagnostics (Burgess Hill, West Sussex, UK). Anti-Rab7 was purchased from Cell Signaling Technologies (Hitchin, Hertfordshire, UK). Anti-Vps45 was bought from Synaptic Systems GmbH (Goettingen, Germany). Anti-prohibitin and anti-calnexin were from Assay Designs and StressGen Biotechnologies (Ann Arbor, MI). HRP-conjugated cholera toxin B subunit, anti-AP1, anti-α1,2-Mannosidase IA, and anti-Rab9 were purchased from Sigma-Aldrich (Poole, Dorset, UK). Anti-PI4KIIIβ antiserum was purchased from Millipore (Watford, UK). Antibody to PI4KIIα was previously described (20). For confocal microscopy, anti-TGN38 was purchased from AbD Serotec (Kidlington, UK), and anti-Rab11 was from Zymed Laboratories (San Francisco). DMEM and FBS were purchased from PAA laboratories (Yeovil, Somerset, UK), and penicillin/streptomycin were purchased from Sigma-Aldrich (Poole, Dorset, UK). [γ-^{32}P]ATP and ECL Western blotting reagents were purchased from GE Healthcare (Little Chalfont, Buckinghamshire, UK). InstantBlue stain was from Expedeon (Cambridgeshire, UK). All other reagents were from Sigma- Aldrich (Poole, Dorset, UK).

Cell culture

A431, HT1080, and COS-7 cells were maintained at 37°C in a humidified incubator at 5% CO_2. Cells were cultured in DMEM containing stable glutamine, 10% fetal bovine serum, 50 IU/ml penicillin, and 50 μg/ml streptomycin.

Subcellular fractionation by discontinuous sucrose density gradient centrifugation

Postnuclear supernatants from cell monolayers were prepared as described previously (17). Typically, confluent monolayers cultured on two to four 14 cm dishes were placed on ice, washed twice with ice-cold PBS (pH 7.4) to remove culture medium, followed by 1 min in ice-cold 10 mM Tris/HCl (pH 7.4) to induce osmotic swelling as an aid to cell disruption. The osmotic buffer was quickly decanted, and the cells were scraped into an ice-cold homogenization buffer composed of 10 mM Tris/HCl, 1 mM EGTA, 0.5 mM EDTA, 0.25 M sucrose (pH 7.4), and Complete™ protease inhibitors (Roche), and then homogenized with ten strokes of a loose-fitting Dounce homogenizer. The disrupted cells were transferred to 1.5 ml polypropylene microcentrifuge tubes. All subsequent steps were carried out at 4°C or on ice. Postnuclear supernatants (PNS) were obtained by centrifugation of the cell homogenate for 10 min at 1,000 *g*. The 1,000 *g* nuclear pellet was resuspended in 1 ml of homogenization buffer, sonicated with a Vibra™Cell probe sonicator (Sonics) at amplitude setting 40 in pulsed mode, and stored as the nuclear pellet fraction. Postnuclear supernatants were centrifuged at 8,000 *g* for 20 min at 4°C in a bench-top centrifuge to pellet the plasma membrane, mitochondria, and rough endoplasmic reticulum. After decanting off the supernatant for sucrose density gradient fractionation, the 8,000 *g* pellet was resuspended in 1 ml of homogenization buffer and sonicated by 3 × 5 s bursts with a Sonics Vibra™cell probe (Sonics) sonicator at amplitude setting 40 operated in pulsed mode and stored as the p8000 pellet fraction. The post-8,000 *g* supernatant was equilibrated in 100 mM sodium carbonate pH 11.0 for 5 min, sonicated by 3 × 5 s bursts with a Vibra-cell probe (Sonics) sonicator at amplitude setting 40 operated in pulsed mode. This sonicated fraction was transferred to a 12 ml polycarbonate ultracentrifuge tube (Beckman) and adjusted to 40% (w/v) sucrose by the addition of an equal volume of 80% (w/v) sucrose in 10 mM Tris-HCl (pH 7.4), 1 mM EDTA, and 1 mM EGTA to give a final volume of 4 ml. The sample was overlaid with 4 ml of 35% (w/v) sucrose, followed by 4 ml of 5% (w/v) sucrose, and subjected to discontinuous equilibrium sucrose density gradient centrifugation overnight at 4°C at 180,000 *g* using a swing-out SW41 Beckman rotor. Then 1 ml gradient fractions were harvested beginning from the top of the tube and stored at −20°C. While the data presented here pertains to overnight ultracentrifugation experiments, trial experiments revealed that it was possible to obtain similar results by reducing the centrifugation time to 4 h.

Subcellular fractionation by continuous sucrose density gradient centrifugation

Postnuclear supernatants, prepared as described in the preceding section, were fractionated on a continuous 10-40% (w/v) sucrose density gradient as previously described (17, 21, 22). PNS samples adjusted to 2 ml were layered on to a sucrose gradient prepared by successive layers of 2 ml 40% (w/v), 2 ml 30%, 2 ml 25%, 2 ml 20%, 1 ml 15%, and 1 ml 10% sucrose in 10 mM Tris/HCl, 1 mM EGTA, and 0.5 mM EDTA (pH 7.4). Gradients were centrifuged overnight at 180,000 *g*. After centrifugation, 12 × 1 ml fractions were harvested, beginning at the top of the gradient.

Immunoblotting and protein analyses

Samples were mixed with an equal volume of 2× sample buffer and separated by SDS-PAGE. Proteins were transferred to polyvinylidene difluoride (PVDF) membranes and probed with various antibodies. Bound antibody was detected using the ECL system (GE Healthcare, Little Chalfont, Buckinghamshire, UK). In separate experiments, the protein content of equal-volume samples was determined by the Bradford assay, and proteins separated by SDS-PAGE were visualized using the colloidal Coomassie InstantBlue stain.

Cholesterol assay

The cholesterol content of equal-volume membrane fractions was assayed using the Amplex red cholesterol assay kit from Molecular Probes (Invitrogen, Paisley, UK).

Detection of GM1 glycosphingolipid. A dot blotting method was employed to establish the gradient distribution of GM1 glycosphingolipid (23). Equal-volume samples of each subcellular fraction were dotted onto nitrocellulose membrane and probed with HRP-conjugated cholera toxin B subunit (1:10,000) to detect GM1 glycosphingolipid using ECL reagents.

Electron microscopy of sonicated membranes. Postnuclear supernatants were probe-sonicated in carbonate buffer as described in preceding sections and separated on a 40-35-5% w/v sucrose density gradient. Buoyant membranes were fixed in suspension in 1% (w/v) OsO_4, pelleted by centrifugation for 30 min in a benchtop centrifuge at maximum setting, stained with 2% (v/v) uranyl acetate for 1 h at 4°C in the dark (24), and then imaged by electron microscopy.

Confocal immunofluorescence studies

COS-7 cells were grown on poly(L)lysine-coated glass coverslips for 24 h and fixed with 4% (v/v) formaldehyde for 10 min on ice. They were then permeabilized in 0.05% Triton X-100 for 5 min on ice, followed by immunostaining with anti-PI4KIIα, anti-syntaxin-6, anti-TGN-38, or anti-Rab11. After counterstaining with Hoechst 33342 (Invitrogen, Paisley, UK), the coverslips were mounted in ProLongGold anti-fade reagent (Invitrogen). Cells were imaged as described previously (25) using a Zeiss LSM 510 Meta laser-scanning confocal microscope system.

RESULTS AND DISCUSSION

Equilibrium density centrifugation results in incomplete organelle separation

Widely used preparations to prepare TGN-enriched membranes result in substantial coenrichment of late endosomal and Golgi-derived membranes and poor separation from lysosomal membranes. To illustrate this, we prepared postnuclear supernatants obtained from HT1080 cells disrupted by a loose-fitting Dounce homogenizer in ice-cold isotonic buffer. The supernatants were separated on a 10-40% (w/v) sucrose gradient by equilibrium density gradient centrifugation. The membranes were found to distribute between fractions 7 and 12, which represent the 20-40% sucrose regions of the gradient (**Fig. 1**). Equal-volume samples from each fraction were assessed for their endomembrane content by Western blotting for organelle-specific marker proteins. Using this approach, we found that the gradient distribution of immunoreactivity against the late endosome-localized proteins syntaxin-8 (26) and Rab9 (27) exhibited substantial overlap with the TGN-targeted glycoprotein TGN38 (28, 29) in fractions 8-10 of the gradient (Fig. 1A). Furthermore, Vps45, a protein that traffics between the TGN and endosomes (30), was poorly resolved from the late endosomal and TGN marker proteins in fractions 9 and 10. We also examined the distribution of the lysosomal marker prenylcysteine lyase (31) and found that while it was mainly confined to the dense fractions 11 and 12, there was also a substantial amount in the TGN and late endosomal fractions. From these data, we infer that widely employed sucrose gradient centrifugation protocols do not clearly separate the TGN from late endosomal membranes or lysosomes. Furthermore, we observed that most of the cellular cholesterol distributed to the dense fractions 11 and 12, with 20-30%

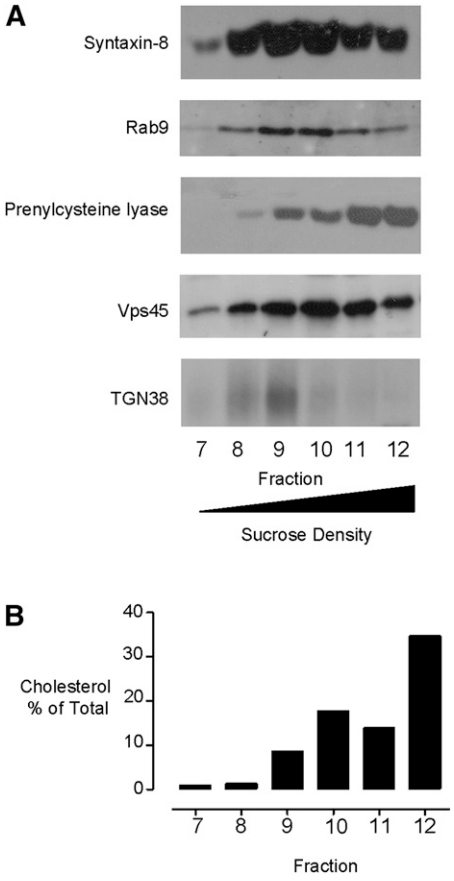

Fig. 1. Subcellular fractionation by equilibrium density gradient centrifugation does not separate different endomembranes. (A) Gradient distributions of late endosomal proteins syntaxin-8 (1:1000) and Rab9 (1:500), lysosomal prenylcysteine lyase (1:1000), Golgi-localized Vps45 (1:500), and TGN-targeted TGN38 (1:1000) were determined by immunoblotting equal volumes of the gradient fractions. (B) Distribution of cholesterol as measured using the Amplex red cholesterol assay. Antibody dilutions used for immunoblotting are in parentheses. TGN, *trans*-Golgi network.

of this lipid localizing to the TGN and late endosomal fractions 8-10 (Fig. 1B). However, due to the poor resolution of different membranes in this preparation, it was not possible to unequivocally determine the amount of cholesterol associated with any individual subcellular compartment. To isolate a purer cholesterol-rich endomembrane fraction, an alternative approach was adopted.

Removal of cholesterol-rich plasma membrane and endoplasmic reticulum from cell homogenates

To improve the separation of cholesterol-rich endomembranes, we devised a strategy with the initial objective of removing the cholesterol-rich plasma membrane. For these experiments, we typically used two 14 cm dishes of confluent cell monolayers. The cells were scraped into an isotonic homogenization buffer followed by gentle Dounce homogenization. A loose-fitting homogenizer was used to minimize vesicularization of larger membranes, such as the plasma membrane and endoplasmic reticulum, to preserve their potential for rapid sedimentation. The resultant cell homogenate was centrifuged at

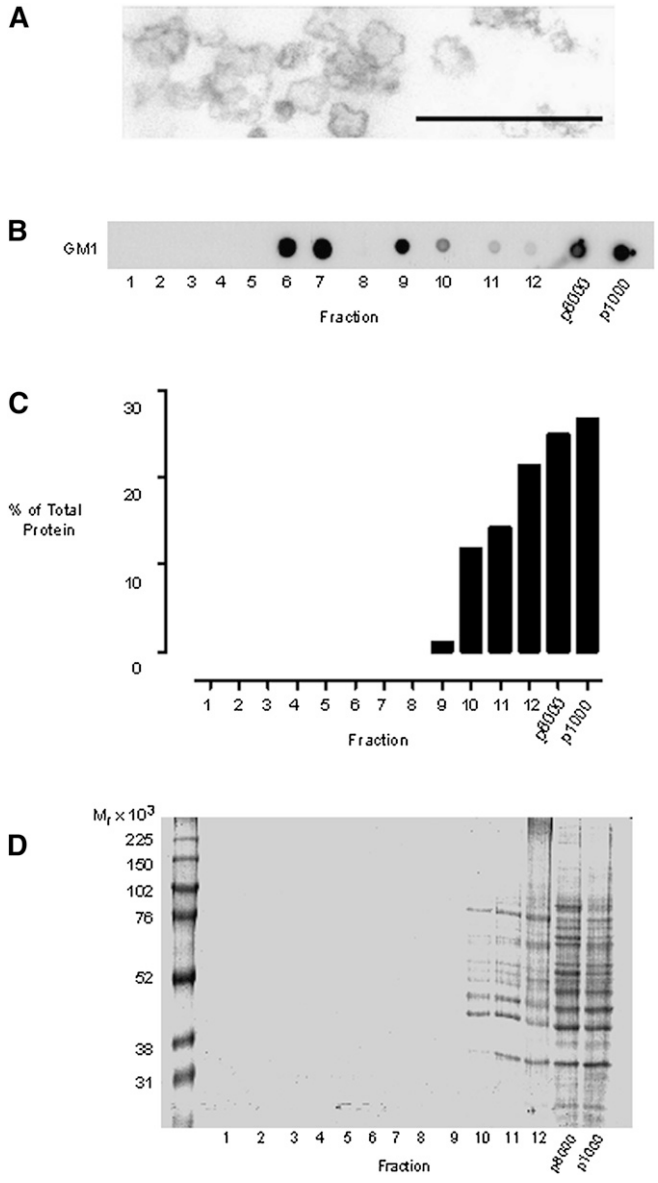

Fig. 2. Detergent-free isolation of a buoyant-membrane fraction enriched for GM1 lipid. Cells were disrupted by gentle Dounce homogenization, and a nuclear pellet obtained by centrifuging the homogenate at 1,000 *g*. The 1,000 *g* pellet was resuspended in 1 ml of homogenization buffer to give the p1000 fraction. The postnuclear supernatant was centrifuged at 8,000 *g* for 20 min, and the pellet was resuspended in 1 ml of homogenization buffer to form the p8000 fraction. The 8,000 *g* supernatant was subjected to carbonate addition, sonicated, and bottom loaded on a 40-35-5% (w/v) discontinuous sucrose gradient. The gradient was subjected to overnight ultracentrifugation, and 12 × 1 ml gradient fractions were collected from the top of the tube. (A) Electron micrograph demonstrating that the probe sonication conditions employed resulted in the generation of vesicles with diameters in the region of 50-200 nm. Scale bar 500 nm. (B) Dot blots showing the gradient distribution of GM1 glycosphingolipid, detected with HRP-conjugated cholera toxin B subunit. (C) Analyses of the protein content of the subcellular fractions using the Bradford assay. (D) Colloidal Coomassie blue staining of SDS-PAGE separated proteins from equal-volume samples from each subcellular fraction.

1,000 *g* for 10 min to remove nuclei and unbroken cells, a standard procedure in many cell fractionation schemes. This gave rise to two cellular fractions: a nuclear p1000 pellet and a postnuclear supernatant. The postnuclear supernatant would be expected to contain all the cytosolic components and nonnuclear membranes released during the cell disruption procedure. Rather than immediately subfractionating the postnuclear supernatant, we decided to include another step to clear the cholesterol-rich plasma membrane. This step was also introduced to remove mitochondria, which often end up as contaminating membranes in lipid microdomain isolation experiments (16). We reasoned that subjecting the postnuclear supernatant to short, intermediate-speed centrifugation might be sufficient to substantially remove large and dense organelles from the postnuclear supernatants, while buoyant and smaller vesicles, such as endosomes, would be less affected. This step gave rise to two further fractions: a p8000 pellet and a post-8,000 *g* supernatant**.** The post-8,000 g supernatant was pulse-sonicated using a probe sonicator to generate submicron membrane fragments. In the absence of detergent, sonication has been employed previously to release cholesterol-rich membrane microdomains, such as caveolae (32), from larger membranes, and we confirmed that these conditions resulted in the generation of 50-200 nm diameter vesicles (**Fig. 2A**). Sonication was carried out in the presence of carbonate, as we previously established

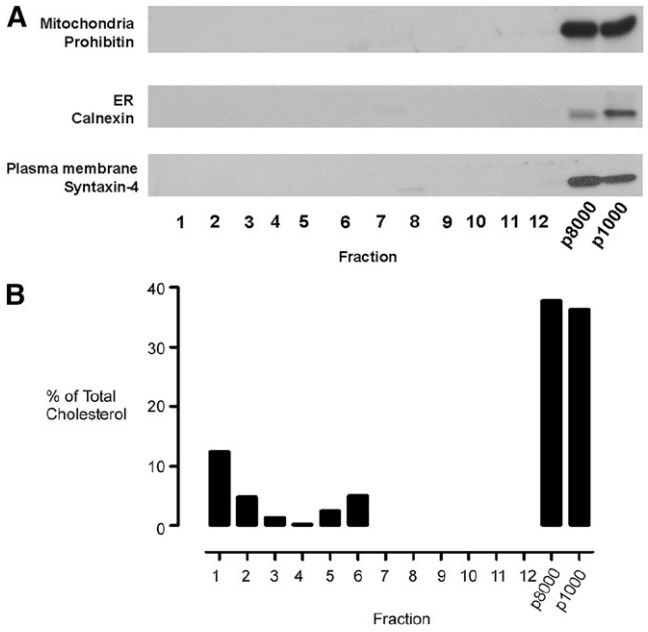

Fig. 3. Preparation of a buoyant cholesterol-rich endomembrane membrane fraction. Equal volumes of all subcellular fractions were subjected to SDS-PAGE separation and immunoblotted for (A) the mitochondrial marker protein prohibitin (1:2000), the ER protein calnexin (1:5000), and the plasma membrane-associated protein syntaxin-4.(1:1000). (B) Distribution of cholesterol as measured using the Amplex red cholesterol assay. Data are presented as percentage of total cholesterol measured across the gradient. Antibody dilutions used are in parentheses. ER, endoplasmic reticulum.

that this minimizes membrane aggregation and facilitates the generation of small vesicles (19, 33). Following sonication, the membranes were separated by equilibrium density centrifugation on a 40-35-5% (w/v) discontinuous sucrose gradient, and 1 ml fractions were collected beginning at the top of the ultracentrifuge tube. Equal-volume samples from each subcellular fraction were subsequently analyzed for their protein and cholesterol content.

Because lipid rafts are characteristically enriched for glycosphingolipids, we dot-blotted for the presence of the GM1 glycosphingolipid using HRP-labeled cholera toxin B subunit. We found that there was a significant pool of GM1 lipid present in the buoyant region of the sucrose gradient at the interface of the 5 and 35% (w/v) sucrose layers, typically found between fractions 5 and 7 (Fig. 2B). When the protein content of each subcellular fraction was assessed using either the Bradford assay or the more sensitive technique of colloidal Coomassie blue staining of SDS-PAGE gels, it was clear that the protein levels of the buoyant lipid-rich fractions were below the detection threshold of either technique (Fig. 2). As the gel-staining technique we used can detect as little as 5-25 ng of protein per band, these analyses led us to infer that the buoyant membrane fraction is highly enriched for lipid relative to protein.

Western blots demonstrated that the plasma membrane marker syntaxin-4 (34), the endoplasmic reticulum resident protein calnexin (35), and the mitochondrial protein prohibitin (36) were all confined to the p1000 and p8000 pellets (**Fig. 3A**). No immunoreactivity against any of these highly expressed proteins could be detected in any of the subsequent fractions prepared by 40-35-5% (w/v) discontinuous sucrose gradient fractionation of the post-8,000 *g* supernatant (Fig. 3A).

As one of the main objectives was to isolate cholesterol-rich endomembranes, we examined the distribution of cholesterol in the different gradient fractions. We found that 5-10% of the cellular cholesterol was found in fractions 5-7, which correspond to the buoyant membrane fractions (Fig. 3). The remaining 70-80% of the total cellular cholesterol was mainly associated with the p8000 plasma membrane-enriched pellet and to a lesser degree with fractions 1-3 of the density gradient. These analyses demonstrated that a simple centrifugal clearance step was extremely effective in removing the plasma membrane, endoplasmic reticulum, and mitochondria from the sample prior to density gradient fractionation, and it facilitated

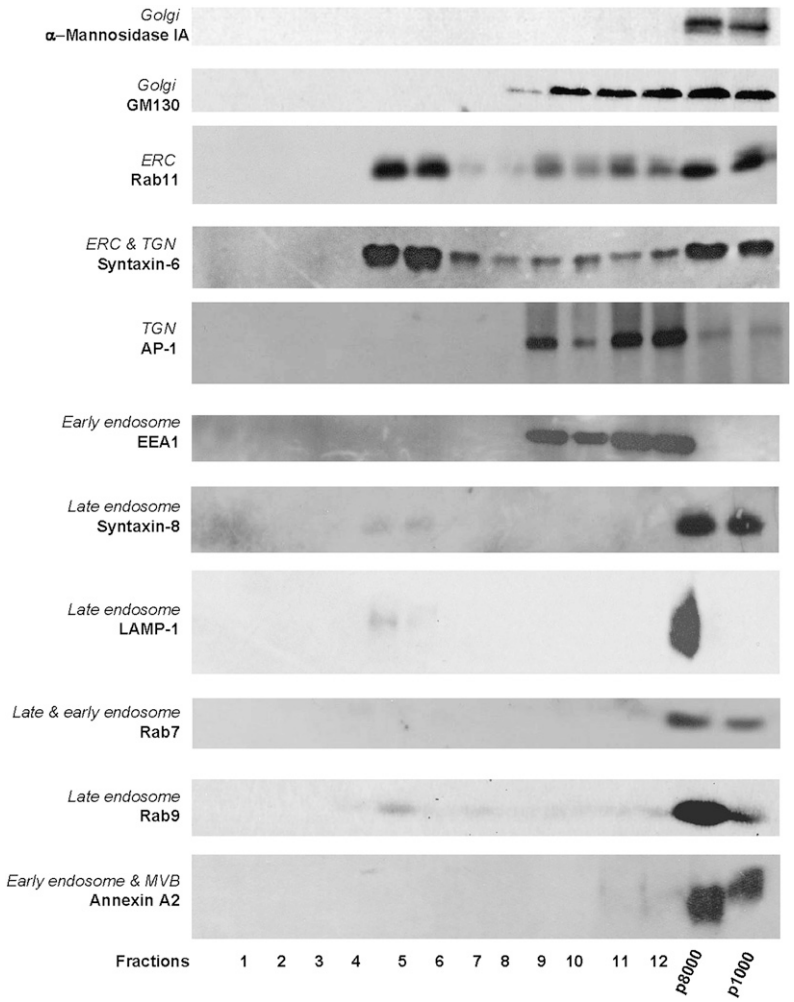

Fig. 4. Distribution of TGN and endosomal membranes in the gradient fractions. Endomembrane fractions were prepared, and equal-volume samples from each gradient fraction were separated by SDS-PAGE and probed by Western blotting against a panel of Golgi and endosomal protein markers. The main subcellular localization of each protein is shown in italics. The antibody dilutions (in parentheses) used for Western blotting were anti-α1,2-mannosidase IA (1:1000), anti-GM130 (1:1000), anti-Rab11 (1:200), anti-syntaxin-6 (1:500), anti-AP-1 (1:500), anti-EEA1 (1:1000), anti-syntaxin-8 (1:1000), anti-LAMP1 (1:1000), anti-Rab7 (1:200), anti-Rab9 (1:100), and anti-Annexin A2 (1:1000). TGN, *trans*-Golgi network. [AQ7]

the subsequent isolation of cholesterol-enriched, low-buoyant-density membranes.

Characterization of the intracellular membrane preparation

Immunoblotting against a range of organelle-specific marker proteins was employed to establish the subcellular origin of the buoyant and cholesterol-rich membrane fraction (**Fig. 4**). We found that the interface between the 5% and 35% sucrose layers, typically found between fractions 5 and 7 of the gradient, contained a peak of immunoreactivity for the TGN and recycling endosome marker Rab11 (37) and the TGN/endosome-associated protein syntaxin-6 (38, 39). A significant proportion of the total cellular content of these two proteins was also found in the p8000 pellet, indicating the existence of biophysically distinct pools. Immunoreactivity for syntaxin-8, a protein involved in late endosomal and TGN trafficking that has been localized to both early (40) and late endosomes (41), was confined largely to the preclearing pellet fractions, but a very small amount did cofractionate with the low-buoyant-density membranes. The pattern of immunoreactivity for Rab7, a small GTPase that localizes mainly to late endosomes (42) and also to the early endosomal compartment, was similar to syntaxin-8, although in the case of Rab7, all immunoreactivity was detected in the p8000 and p1000 pellets, with no immunoreactivity observed in the buoyant fraction. The lysosomal and late endosomal glycoprotein LAMP-1 exhibited a similar distribution to syntaxin-8, being mainly confined to the p8000 fraction, with very weak immunoreactivity present between the 5% and 35% sucrose layer interface. Annexin A2 associates with early endosomes (43) and has been implicated in the biogenesis of multivesicular bodies. We found that, similar to Rab7, annexin A2 was also confined to the p8000 and p1000 fractions. This is

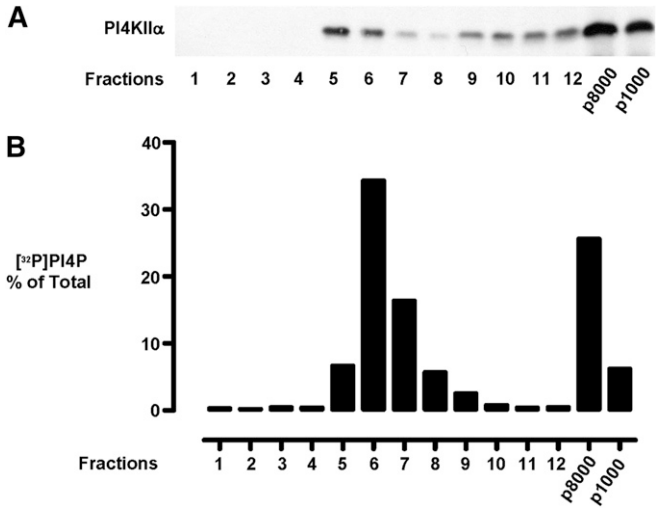

Fig. 5. Distribution of PI4KIIα and PI4P synthesis in the subcellular fractions. Endomembrane fractions were prepared. and equal-volume samples from each gradient fraction were separated by SDS-PAGE and probed by Western blotting against (A) PI4KIIα (1:5 hybridoma culture supernatant) and (B) distribution of PI4P synthesis in the gradient fractions. PI4P, phosphatidylinositol 4-phosphate; PI4KII, type II phosphatidylinositol 4-kinase.

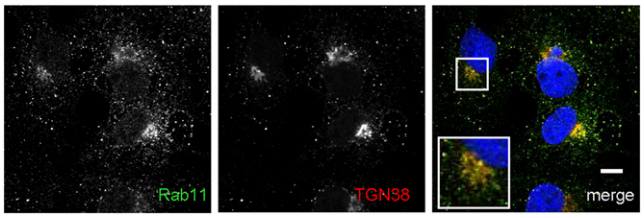

Fig. 6. Immunofluorescence studies reveal colocalization of Rab11 and TGN38 on small vesicles. COS-7 cells were fixed and stained with antibodies against Rab11 (green) and TGN38 (red). Scale bar is 10 μm. Boxed area is magnified to show colocalization in the juxtanuclear region. TGN, *trans*-Golgi network.

further evidence that early endosomes are not present in the buoyant membrane fraction. Immunoblotting against the TGN-recruited adaptor protein AP-1 (44) and the early endosome-recruited protein EEA1 (45) revealed that both proteins were localized to the dense fractions 8-12. Finally, the *cis*-Golgi marker GM130 (46) was enriched in the p8000 fraction and to a lesser degree the dense fractions 8-12. The removal of *cis*-Golgi membranes was confirmed by immunoblotting against the Golgi protein α1,2-mannosidase IA (47, 48), as immunoreactivity against this protein was confined to the p8000 and p1000 nongradient fractions. These results demonstrate effective clearance of Golgi stacks from the buoyant, cholesterol-rich membranes. The partial separation of TGN and *cis*-Golgi membranes in this fractionation scheme is significant as there is a previous demonstration that markers from both these compartments partially overlap throughout the *cis*, medial, and *trans*-Golgi stacks (49). However, the post-Golgi, highly tubular and vesicular TGN, which was absent from the membrane preparation used in the study by Taguchi et al. (49), is the subcellular membrane enriched in the buoyant fraction described here.

Distribution of PI4P synthesis and PI4KIIα

To illustrate a use for this procedure, we employed it to investigate the subcellular localization of the lipid kinase PI4KIIα, which catalyses the conversion of phosphatidylinositol to phosphatidylinositol 4-phosphate (PI4P). This enzyme has been localized in immunofluorescence studies both to late endosomes (25, 50) and the TGN (44), where it is required for the recruitment of AP-1 (44) and AP-3 (50) adaptor proteins, respectively. However, there are some disagreements concerning the definitive steady state localization of the enzyme, and our previous work has revealed the existence of PI4KIIα pools of differing intrinsic activity (17, 21). To elucidate which subcellular membrane is the main subcellular site for PI4P synthesis, we utilized the membrane fractionation procedure described here to compare the distribution of PI4KIIα protein with the distribution of PI4P synthesis using membrane-associated, endogenous phosphatidylinositol substrate, which reports PI4KIIα activity (20, 22, 51). This revealed a peak of [^{32}P]PI4P generation, amounting to 50-60% of the cellular total, in a buoyant membrane fraction situated in the cholesterol-rich fractions 5-7 of the gradient (**Fig. 5**). As Western blotting of the gradient fractions

(Fig. 5) revealed that more PI4KIIα protein was present in the p8000 late-endosome enriched pellet than in the buoyant interface fractions, we infer that the buoyant pool of PI4KIIα corresponds to the active pool of the enzyme we described previously (21). Therefore, in this example, this new fractionation scheme permits an assessment of the relative levels of PI4KIIα and PI4P synthesis on different endomembranes and also the degree to which PI4P synthesis is compartmentalized on endomembrane microdomains.

Immunofluorescence analyses

Our immunoblotting analyses suggested that there may be colocalization between TGN and recycling endosome markers, which given the intrinsic buoyancy of these membranes and their resistance to sedimentation at 8,000 *g*, was likely to occur on small vesicles. On the other hand, there was also a possibility that the cofractionation of TGN and recycling markers could have resulted from sonication-induced membrane fusion. We investigated these scenarios with confocal immunofluorescence studies to visualize the localizations of Rab11 and TGN38 in fixed cells. We found partial overlap between these proteins on juxtanuclear puncta (**Fig. 6**) and on small peripheral vesicles. Colocalization of Rab11 and TGN38 on small peripheral vesicles suggests that our subcellular fractionation strategy results in significant enrichment of a subset of post-Golgi-trafficking vesicles (52). We conclude that the buoyant membrane fraction consists of cholesterol-rich membrane domains that originate from TGN vesicles or endosome-TGN intermediates (reviewed in Ref. 53). Therefore, this straightforward subcellular fractionation method facilitates a rapid, detergent-free isolation of lipid-rich membrane domains from these highly dynamic trafficking vesicles and can be used to provide insights into the subcellular compartmentalization of lipid metabolism and vesicular trafficking.

The authors thank the Electron Microscopy Unit of the Royal Free Hampstead NHS Trust Hospital for its contribution to this study.

REFERENCES

1. Mukherjee, S., X. Zha, I. Tabas, and F. R. Maxfield. 1998. Cholesterol distribution in living cells: fluorescence imaging using dehydroergosterol as a fluorescent cholesterol analog. *Biophys. J.* **75:** 1915–1925.
2. Mobius, W., E. van Donselaar, Y. Ohno-Iwashita, Y. Shimada, H. F. Heijnen, J. W. Slot, and H. J. Geuze. 2003. Recycling compartments and the internal vesicles of multivesicular bodies harbor most of the cholesterol found in the endocytic pathway. *Traffic.* **4:** 222–231.
3. Chang, T. Y., P. C. Reid, S. Sugii, N. Ohgami, J. C. Cruz, and C. C. Chang. 2005. Niemann-Pick type C disease and intracellular cholesterol trafficking. *J. Biol. Chem.* **280:** 20917–20920.
4. Vance, J. E. 2006. Lipid imbalance in the neurological disorder, Niemann-Pick C disease. *FEBS Lett.* **580:** 5518–5524.
5. Maxfield, F. R., and I. Tabas. 2005. Role of cholesterol and lipid organization in disease. *Nature.* **438:** 612–621.
6. Choudhury, A., D. K. Sharma, D. L. Marks, and R. E. Pagano. 2004. Elevated endosomal cholesterol levels in Niemann-Pick cells inhibit rab4 and perturb membrane recycling. *Mol. Biol. Cell.* **15:** 4500–4511.
7. Lebrand, C., M. Corti, H. Goodson, P. Cosson, V. Cavalli, N. Mayran, J. Faure, and J. Gruenberg. 2002. Late endosome motility depends on lipids via the small GTPase Rab7. *EMBO J.* **21:** 1289–1300.
8. Choudhury, A., M. Dominguez, V. Puri, D. K. Sharma, K. Narita, C. L. Wheatley, D. L. Marks, and R. E. Pagano. 2002. Rab proteins mediate Golgi transport of caveola-internalized glycosphingolipids and correct lipid trafficking in Niemann-Pick C cells. *J. Clin. Invest.* **109:** 1541–1550.
9. Linder, M. D., R. L. Uronen, M. Holtta-Vuori, P. van der Sluijs, J. Peranen, and E. Ikonen. 2007. Rab8-dependent recycling promotes endosomal cholesterol removal in normal and sphingolipidosis cells. *Mol. Biol. Cell.* **18:** 47–56.
10. Ganley, I. G., and S. R. Pfeffer. 2006. Cholesterol accumulation sequesters Rab9 and disrupts late endosome function in NPC1-deficient cells. *J. Biol. Chem.* **281:** 17890–17899.
11. Vainio, S., and E. Ikonen. 2003. Macrophage cholesterol transport: a critical player in foam cell formation. *Ann. Med.* **35:** 146–155.
12. Brusselmans, K., L. Timmermans, T. Van de Sande, P. P. Van Veldhoven, G. Guan, I. Shechter, F. Claessens, G. Verhoeven, and J. V. Swinnen. 2007. Squalene synthase, a determinant of raft-associated cholesterol and modulator of cancer cell proliferation. *J. Biol. Chem.* **282:** 18777–18785.
13. Pediconi, M. F., C. E. Gallegos, E. B. De Los Santos, and F. J. Barrantes. 2004. Metabolic cholesterol depletion hinders cell-surface trafficking of the nicotinic acetylcholine receptor. *Neuroscience.* **128:** 239–249.
14. Sugii, S., S. Lin, N. Ohgami, M. Ohashi, C. C. Chang, and T. Y. Chang. 2006. Roles of endogenously synthesized sterols in the endocytic pathway. *J. Biol. Chem.* **281:** 23191–23206.
15. Waugh, M. G., and J. J. Hsuan. 2009. Preparation of membrane rafts. *Methods Mol. Biol.* **462:** 403–414.
16. Zheng, Y. Z., K. B. Berg, and L. J. Foster. 2009. Mitochondria do not contain lipid rafts, and lipid rafts do not contain mitochondrial proteins. *J. Lipid Res.* **50:** 988–998.
17. Waugh, M. G., S. Minogue, J. S. Anderson, A. Balinger, D. Blumenkrantz, D. P. Calnan, R. Cramer, and J. J. Hsuan. 2003. Localization of a highly active pool of type II phosphatidylinositol 4-kinase in a p97/valosin-containing-protein-rich fraction of the endoplasmic reticulum. *Biochem. J.* **373:** 57–63.
18. Song, K. S., S. Li, T. Okamoto, L. A. Quilliam, M. Sargiacomo, and M. P. Lisanti. 1996. Co-purification and direct interaction of Ras with caveolin, an integral membrane protein of caveolae microdomains. Detergent-free purification of caveolae microdomains. *J. Biol. Chem.* **271:** 9690–9697.
19. Waugh, M. G., D. Lawson, and J. J. Hsuan. 1999. Epidermal growth factor receptor activation is localized within low-buoyant density, non-caveolar membrane domains. *Biochem. J.* **337:** 591–597.
20. Simons, J. P., R. Al-Shawi, S. Minogue, M. G. Waugh, C. Wiedemann, S. Evangelou, A. Loesch, T. S. Sihra, R. King, T. T. Warner, et al. 2009. Loss of phosphatidylinositol 4-kinase 2alpha activity causes late onset degeneration of spinal cord axons. *Proc. Natl. Acad. Sci. USA.* **106:** 11535–11539.
21. Waugh, M. G., S. Minogue, D. Blumenkrantz, J. S. Anderson, and J. J. Hsuan. 2003. Identification and characterization of differentially active pools of type IIalpha phosphatidylinositol 4-kinase activity in unstimulated A431 cells. *Biochem. J.* **376:** 497–503.
22. Waugh, M. G., S. Minogue, D. Chotai, F. Berditchevski, and J. J. Hsuan. 2006. Lipid and peptide control of phosphatidylinositol 4-kinase IIalpha activity on Golgi-endosomal rafts. *J. Biol. Chem.* **281:** 3757–3763.
23. Ilangumaran, S., S. Arni, Y. Chicheportiche, A. Briol, and D. C. Hoessli. 1996. Evaluation by dot-immunoassay of the differential distribution of cell surface and intracellular proteins in glycosylphosphatidylinositol-rich plasma membrane domains. *Anal. Biochem.* **235:** 49–56.
24. Stan, R. V., W. G. Roberts, D. Predescu, K. Ihida, L. Saucan, L. Ghitescu, and G. E. Palade. 1997. Immunoisolation and partial characterization of endothelial plasmalemmal vesicles (caveolae). *Mol. Biol. Cell.* **8:** 595–605.
25. Minogue, S., M. G. Waugh, M. A. De Matteis, D. J. Stephens, F. Berditchevski, and J. J. Hsuan. 2006. Phosphatidylinositol 4-kinase is required for endosomal trafficking and degradation of the EGF receptor. *J. Cell Sci.* **119:** 571–581.
26. He, Y., and M. E. Linder. 2009. Differential palmitoylation of the endosomal SNAREs syntaxin 7 and syntaxin 8. *J. Lipid Res.* **50:** 398–404.

27. Lombardi, D., T. Soldati, M. A. Riederer, Y. Goda, M. Zerial, and S. R. Pfeffer. 1993. Rab9 functions in transport between late endosomes and the trans Golgi network. *EMBO J.* **12:** 677–682.
28. Luzio, J. P., B. Brake, G. Banting, K. E. Howell, P. Braghetta, and K. K. Stanley. 1990. Identification, sequencing and expression of an integral membrane protein of the trans-Golgi network (TGN38). *Biochem. J.* **270:** 97–102.
29. Ponnambalam, S., M. Girotti, M. L. Yaspo, C. E. Owen, A. C. Perry, T. Suganuma, T. Nilsson, M. Fried, G. Banting, and G. Warren. 1996. Primate homologues of rat TGN38: primary structure, expression and functional implications. *J. Cell Sci.* **109:** 675–685.
30. Tellam, J. T., D. E. James, T. H. Stevens, and R. C. Piper. 1997. Identification of a mammalian Golgi Sec1p-like protein, mVps45. *J. Biol. Chem.* **272:** 6187–6193.
31. Tschantz, W. R., L. Zhang, and P. J. Casey. 1999. Cloning, expression, and cellular localization of a human prenylcysteine lyase. *J. Biol. Chem.* **274:** 35802–35808.
32. Smart, E. J., Y. S. Ying, C. Mineo, and R. G. Anderson. 1995. A detergent-free method for purifying caveolae membrane from tissue culture cells. *Proc. Natl. Acad. Sci. USA.* **92:** 10104–10108.
33. Waugh, M. G., D. Lawson, S. K. Tan, and J. J. Hsuan. 1998. Phosphatidylinositol 4-phosphate synthesis in immunoisolated caveolae-like vesicles and low buoyant density non-caveolar membranes. *J. Biol. Chem.* **273:** 17115–17121.
34. Fujita, H., P. L. Tuma, C. M. Finnegan, L. Locco, and A. L. Hubbard. 1998. Endogenous syntaxins 2, 3 and 4 exhibit distinct but overlapping patterns of expression at the hepatocyte plasma membrane. *Biochem. J.* **329:** 527–538.
35. Ahluwalia, N., J. J. Bergeron, I. Wada, E. Degen, and D. B. Williams. 1992. The p88 molecular chaperone is identical to the endoplasmic reticulum membrane protein, calnexin. *J. Biol. Chem.* **267:** 10914–10918.
36. Ikonen, E., K. Fiedler, R. G. Parton, and K. Simons. 1995. Prohibitin, an antiproliferative protein, is localized to mitochondria. *FEBS Lett.* **358:** 273–277.
37. Ullrich, O., S. Reinsch, S. Urbe, M. Zerial, and R. G. Parton. 1996. Rab11 regulates recycling through the pericentriolar recycling endosome. *J. Cell Biol.* **135:** 913–924.
38. Bock, J. B., J. Klumperman, S. Davanger, and R. H. Scheller. 1997. Syntaxin 6 functions in trans-Golgi network vesicle trafficking. *Mol. Biol. Cell.* **8:** 1261–1271.
39. Otto, G. P., M. Razi, J. Morvan, F. Stenner, and S. A. Tooze. 2010. A novel syntaxin 6-interacting protein, SHIP164, regulates syntaxin 6-dependent sorting from early endosomes. *Traffic.* **11:** 688–705.
40. Subramaniam, V. N., E. Loh, H. Horstmann, A. Habermann, Y. Xu, J. Coe, G. Griffiths, and W. Hong. 2000. Preferential association of syntaxin 8 with the early endosome. *J. Cell Sci.* **113:** 997–1008.
41. He, Y., and M. E. Linder. 2009. Differential palmitoylation of the endosomal SNAREs syntaxin 7 and syntaxin 8. *J. Lipid Res.* **50:** 398–404.
42. Chavrier, P., R. G. Parton, H. P. Hauri, K. Simons, and M. Zerial. 1990. Localization of low molecular weight GTP binding proteins to exocytic and endocytic compartments. *Cell.* **62:** 317–329.
43. Emans, N., J. P. Gorvel, C. Walter, V. Gerke, R. Kellner, G. Griffiths, and J. Gruenberg. 1993. Annexin II is a major component of fusogenic endosomal vesicles. *J. Cell Biol.* **120:** 1357–1369.
44. Wang, Y. J., J. Wang, H. Q. Sun, M. Martinez, Y. X. Sun, E. Macia, T. Kirchhausen, J. P. Albanesi, M. G. Roth, and H. L. Yin. 2003. Phosphatidylinositol 4 phosphate regulates targeting of clathrin adaptor AP-1 complexes to the Golgi. *Cell.* **114:** 299–310.
45. Mu, F. T., J. M. Callaghan, O. Steele-Mortimer, H. Stenmark, R. G. Parton, P. L. Campbell, J. McCluskey, J. P. Yeo, E. P. Tock, and B. H. Toh. 1995. EEA1, an early endosome-associated protein. EEA1 is a conserved alpha-helical peripheral membrane protein flanked by cysteine "fingers" and contains a calmodulin-binding IQ motif. *J. Biol. Chem.* **270:** 13503–13511.
46. Nakamura, N., C. Rabouille, R. Watson, T. Nilsson, N. Hui, P. Slusarewicz, T. E. Kreis, and G. Warren. 1995. Characterization of a cis-Golgi matrix protein, GM130. *J. Cell Biol.* **131:** 1715–1726.
47. Herscovics, A. 1999. Importance of glycosidases in mammalian glycoprotein biosynthesis. *Biochim. Biophys. Acta.* **1473:** 96–107.
48. Velasco, A., L. Hendricks, K. W. Moremen, D. R. Tulsiani, O. Touster, and M. G. Farquhar. 1993. Cell type-dependent variations in the subcellular distribution of alpha-mannosidase I and II. *J. Cell Biol.* **122:** 39–51.
49. Taguchi, T., M. Pypaert, and G. Warren. 2003. Biochemical subfractionation of the mammalian Golgi apparatus. *Traffic.* **4:** 344–352.
50. Craige, B., G. Salazar, and V. Faundez. 2008. Phosphatidylinositol-4-Kinase Type II Alpha contains an AP-3 sorting motif and a kinase domain that are both required for endosome traffic. *Mol. Biol. Cell.* **19:** 1415–1426.
51. Waugh, M. G., S. Minogue, and J. J. Hsuan. 2009. Quantification of multiple phosphatidylinositol 4-kinase isozyme activities in cell extracts. *Methods Mol. Biol.* **462:** 279–289.
52. Urbe, S., L. A. Huber, M. Zerial, S. A. Tooze, and R. G. Parton. 1993. Rab11, a small GTPase associated with both constitutive and regulated secretory pathways in PC12 cells. *FEBS Lett.* **334:** 175–182.
53. De Matteis, M. A., and A. Luini. 2008. Exiting the Golgi complex. *Nat. Rev. Mol. Cell Biol.* **9:** 273–284.